AECL--10950
COG--93-376

CA9400039

AECL-10950
COG-93-376

ATOMIC ENERGY OF CANADA LIMITED

ÉNERGIE ATOMIQUE DU CANADA LIMITÉE

MITIGATION OF HARMFUL EFFECTS OF WELDS IN ZIRCONIUM ALLOY COMPONENTS

ATTÉNUATION DES EFFETS NUISIBLES DES SOUDURES D'ÉLÉMENTS FAIT D'ALLIAGES DE ZIRCONIUM

C.E. COLEMAN, G.L. DOUBT, R.W.L. FONG, J.H. ROOT, J.W. BOWDEN, S. SAGAT and R.T. WEBSTER

Presented at 10th International Symposium on Zirconium in the Nuclear Industry, Baltimore, MD, 1993 June 21-24.

Chalk River Laboratories

Laboratoires de Chalk River

Chalk River, Ontario K0J 1J0

October 1993 octobre

AECL Research

MITIGATION OF HARMFUL EFFECTS OF WELDS IN ZIRCONIUM ALLOY COMPONENTS

by

C.E. Coleman, G.L. Doubt, R.W.L. Fong, J.H. Root,
J.W. Bowden, S. Sagat and R.T. Webster*

Presented at 10th International Symposium on Zirconium in the Nuclear Industry, Baltimore, MD, 1993 June 21-24.

AECL Research
Chalk River Laboratories
Chalk River, Ontario
KOJ 1JO

*Metallurgical Consultant
36088 Tree Farm Road
Scio, Oregon 97374

1993 October

AECL-10950
COG-93-376

EACL Recherche

ATTÉNUATION DES EFFETS NUISIBLES DES SOUDURES D'ÉLÉMENTS FAIT D'ALLIAGES DE ZIRCONIUM

par

C.E.Coleman, G.L. Doubt, R.W.L. Fong, J.H. Root,
J.W. Bowden, S. Sagat et R.T. Webster*

RÉSUMÉ

La soudure produit des contraintes de tension résiduelles locales et des changements de texture dans les éléments faits d'alliages de zirconium. Dans les zones affectées thermiquement de tubes ou tôles, les pôles du plan basal sont tournées dans le plan de l'élément et perpendiculaires à la direction de la soudure. Les tubes de Zircaloy-2 à paroi fine comportant une soudure axiale n'atteignent pas une pleine résistance à la rupture du fait qu'ils se rompent toujours prématurément à l'endroit de la soudure lorsqu'on les met sous pression jusqu'à la rupture lors d'un essai de rupture sur tube à bouts encastrés. Le renforcement de la soudure en augmentant son épaisseur de 25% entraîne la rupture du métal de base, améliore la résistance biaxe du tube de 20 à 25% et augmente l'allongement total de 200 à 450%. Dans les éléments faits d'alliage de Zr-2,5Nb, la texture de la zone affectée thermiquement favorise la fissuration par hydruration retardée (DHC) entraînée par les contraintes de tension résiduelles. Bien que la texture ne soit pas beaucoup affectée par les traitements thermiques au-dessous de 630°C et que les contraintes élevées d'interaction des grains persistent du fait des textures mixtes, on peut relaxer les contraintes de tension macrorésiduelles par traitement thermique au point où la probabilité de fissuration sera très faible.

EACL Recherche
Laboratoires de Chalk River
Chalk River (Ontario)
K0J 1J0

*Consultant en métallurgie
36088 Tree Farm Road
Scio, Oregon 97374

1993 octobre

AECL-10950
COG-93-376

AECL Research

MITIGATION OF HARMFUL EFFECTS OF WELDS IN ZIRCONIUM ALLOY COMPONENTS

by

C.E. Coleman, G.L. Doubt, R.W.L. Fong, J.H. Root,
J.W. Bowden, S. Sagat and R.T. Webster*

ABSTRACT

Welding produces local residual tensile stresses and changes in texture in components made from zirconium alloys. In the heat-affected zone in tubes or plates, the basal plane normals are rotated into the plane of the component and perpendicular to the direction of the weld. Thin-walled Zircaloy-2 tubes containing an axial weld do not reach their full strength, because they always fail prematurely in the weld when pressurised to failure in a fixed-end burst test. Reinforcing the weld by increasing its thickness by 25% moves the failure to the parent metal, improves the biaxial strength of the tube by 20 to 25%, and increases the total elongation by 200 to 450%. In components made from Zr-2.5Nb, the texture in the heat-affected zone promotes delayed hydride cracking (DHC) driven by tensile residual stress. Although the texture is not much affected by heat-treatments below 630°C and large grain interaction stresses remain as a result of mixed textures, macro-residual tensile stresses can be relieved by heat-treatment to the point where the probability of cracking is very low.

AECL Research
Chalk River Laboratories
Chalk River, Ontario
KOJ 1JO

*Metallurgical Consultant
36088 Tree Farm Road
Scio, Oregon 97374

1993 October

AECL-10950
COG-93-376

VALUE AND IMPLICATIONS

The harmful effects of welding on the mechanical properties of zirconium alloys due to adverse crystallographic texture or high residual tensile stresses can be mitigated. In Zircaloy-2 calandria tubes, changes in tube geometry will provide extra strength and ductility to increase the margin against the consequences of pressure tube rupture. Heat-treatment of welds in Zr-2.5Nb pressure tubes much reduces the propensity to cracking, thus removing one objection to the use of welds in-reactor.

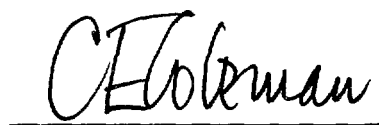

C.E. Coleman

AECL Research
Chalk River Laboratories
Chalk River, Ontario
KOJ 1JO

1993 October

AECL-10950
COG-93-376

1. INTRODUCTION

Welding zirconium produces residual stresses and local changes in microstructure and crystallographic texture. Any use of a welded component has to take these features into account because they affect properties and thus behaviour. Many nuclear components made from zirconium alloys, such as fuel and support structures, are welded and perform with few problems. In this paper we describe two applications:

- the calandria tubes in the CANDU* reactor have given exemplary service, but to increase margins we would like to improve their strength, and
- some pressure tubes are welded and must be protected from delayed hydride cracking (DHC).

2. ZIRCALOY-2 CALANDRIA TUBE

In the fuel channel of a CANDU reactor, the calandria tube surrounds the hot pressure tube and isolates it from the cool heavy-water moderator. The gap between the two tubes is filled with circulating dry CO_2 that acts as an insulator and, in the event of a through-wall crack in the pressure tube, provides a leak detection system. The calandria tube controls the sag of the fuel channel; as demonstrated in Unit 2 of Pickering Nuclear Generating Station, the calandria tube may also contain the pressure of the heat-transport fluid when a pressure tube ruptures [1]. We are exploring ways to strengthen the calandria tubes to increase the margin on the consequences of a failed pressure tube. Thus the strength being addressed is the burst strength of the tube when it is internally pressurised rapidly, rather than the creep strength.

To manufacture calandria tubes, annealed Zircaloy-2 strip is brake-formed and seam-welded [1]. The tubes are 6 m long, have an inside diameter of 130 mm and a wall thickness of 1.4 mm. They normally operate at a temperature of about 70°C, but when exposed to the heat-transport fluid the average temperature is raised to about 170°C. The tubes are firmly attached to the ends of the reactor structure, and when pressurised are stressed in fixed-end mode. The importance of fixed-end biaxial stressing is that it provides a large amount of texture strengthening. The basal plane normals are highly concentrated in the plane perpendicular to the axial direction and, depending on the fabrication route, are localised between 0 and 40° from the thickness direction in the sheet from which the tubes are made. As a result, the material is highly anisotropic. By applying Hill's analysis [2] to fixed-end stressing, we find [3] that the biaxial strength, σ_H, is predicted to be related to the uniaxial strength, U, through:

$$\sigma_H = U_A \sqrt{\frac{(1+R)^2 P}{R(1+R+P)}} \qquad (1)$$

$$= U_T \sqrt{\frac{(1+R)(1+P)}{(1+R+P)}} \qquad (2)$$

The subscripts A and T denote the axial and transverse directions. The anisotropy factor R is determined from the dimensions of longitudinal tensile specimens:

---

* CANDU: CANada Deuterium Uranium; registered trademark.

$$R = \frac{\ln(w/w_o)}{\ln(t/t_o)}$$

The width and thickness of the tensile specimen are written w and t; the subscript o indicates an initial dimension. The anisotropy factor P is similarly determined from transverse tensile specimens. With R and P in the range 2 to 7, we expect a biaxial strength between 35 and 80% greater than the uniaxial strength.

Tubes always fail along the weld in fixed-end burst tests (Appendix A) on both irradiated and unirradiated tubes. Comparison of uniaxial and biaxial strengths (Table I) shows that the full texture strengthening is not realised, even though the weld has a higher strength than the main body of the tube. The texture of the welds has been evaluated by neutron diffraction (Appendix B). The high concentration of basal plane normals in the radial direction, the source of the texture strengthening, is much reduced in the weld, Figure 1, and in biaxial stressing provides the weak link by allowing wall thinning, which leads to rupture. We have examined methods of strengthening calandria tubes, and concluded that to maintain the minimum quantity of parasitic material without destroying the current excellent properties we have to concentrate on eliminating the effect of the weld. The potential improvement in strength can be estimated as the ratio of the full texture strengthening to the biaxial strength of the weld, assuming it to be isotropic:

$$\textit{potential improvement} = \frac{\sigma_H}{1.15\,\sigma_u^w} \qquad (3)$$

where σ_u^w is the uniaxial strength of the weld. Applying Equation (3) to the data in Table I suggests that, if the tube fails outside the weld, an improvement in strengthening of at least 10% should be achievable, with values as high as 40% being possible.

Two potential methods for achieving this extra strength are to thicken the weld or make seamless tubes. To produce a thick weld we have chosen to use uniform strip that is thicker than that currently used, fabricate the tube with present methods, and then remove the excess material to the desired thickness, except for the weld. The aim of the test program was to measure how thick the weld had to be to ensure failure in the main body of the tube, and then evaluate the benefit provided by the change in fabrication route. Prototype seamless tubes have been made by roll-extrusion [4,5].

2.1 Welded Tubes

The material and the tubes used in these tests were made at four different times, by two strip suppliers but by a single tube fabricator. Three orders of tubes had a concentration of basal plane normals about 40° from the radial direction and an oxygen concentration of 0.74 at% (1300 ppm by weight); this material is called Sample 1. In the fourth order of tubes, the basal plane normals were concentrated close to the radial direction, but the oxygen concentration was 0.69 at% (1200 ppm); this material was called Sample 2.

Test specimens were made from standard calandria tubes by dissolving material, in a pickling solution of 3% HF, 15% HNO_3 and 82% H_2O, from the outside of the wall everywhere, except along a 50 mm band centered on the longitudinal seam weld. Thus a weld of thickness w_w was reinforced with respect to the rest of the tube of reduced thickness w_r. The

reinforcement, $(w_w/w_r - 1) \times 100$, was up to 40%. The specimens were pressurised to rupture in a fixed-end biaxial test (Appendix A) at 170°C. The hoop stress and strain at burst are plotted as a function of weld reinforcement in Figure 2 for Sample 1. The lowest reinforcement that caused some specimens to rupture in the parent material was 17%, while specimens with 22% reinforcement could still fail in the weld. On average, specimens that ruptured in the parent material reached a hoop stress about 25% higher than specimens with no weld reinforcement (Table I), confirming the promise of Equation (3). They also reached a hoop strain almost three times as high as that obtained with uniform wall tube. The strain results were variable and this is attributable to increasing sensitivity to small flaws at high strains and variation in the wall thickness from pickling.

A smaller number of tests was done on the tubing made from Sample 2. This material had a sharper texture than Sample 1, but its maximum strengths (Table I), with or without weld reinforcement, were similar to those in Figure 2. The average improvement to the strength by thickening the weld of these calandria tubes was about 21%. The hoop strains to rupture were much different:

Average Hoop Strain at Burst
(no. of specimens in parentheses)

	Sample 1 (Figure 2)	Sample 2 (sharp radial texture)
unreinforced, rupture in weld	7.9 (14)	1.9 (12)
reinforced, rupture in parent material	23.2 (11)	10.4 (3)

The low strain values for the unreinforced tubes in Sample 2 are a result of the large difference in texture between the weld and parent material. With weld reinforcement, the hoop strain increased 450% in Sample 2, but it was still 55% lower than that of Sample 1.

The maximum hoop stresses generated in fixed end burst tests were greater than the transverse uniaxial tensile strength by about 110% in Sample 1 and 120% in Sample 2. A similar comparison for the axial uniaxial tensile strength gives values of 93% and 107% for Sample 1 and Sample 2, respectively. These factors are greater than predicted by Hill's analysis, but we have not determined whether the cause of the discrepancy lies in the limitations of theory when applied at such large strains, whether the values of R and P are large enough, or whether the assumed stress state is fully applicable for the experimental method.

The weld reinforcement, achieved by postponing the tube rupture until the parent material fails, has allowed realization of the full texture strengthening. From the results of the experiments, a difference in thickness between the weld and parent metal of 25% is recommended. The increase in hoop strain obtained by weld reinforcement is a bonus, since it can be of substantial practical benefit. It improves tolerance to the waterhammer-type loading that may occur in certain postulated accidents, and creates a large margin for loss of ductility from neutron irradiation.

2.2 Seamless Tubes

Prototype seamless tubes have been made by roll-extrusion. The fabrication sequence begins with extrusion of a hollow billet at 650°C, followed by externally roll-extruding the annealed hollow, vacuum annealing at 700°C for 1.5 h, then internally roll-extruding the tube to final dimensions. The tubes were given a final vacuum anneal of 750°C for 0.5 h. The finished tube contained equiaxed grains (6-9 μm), with their basal plane normals predominately aligned along the radial direction of the tube.

The effect of a weld on burst strength was determined by testing two samples taken from the seamless tube, where one sample contained a simulated longitudinal weld and the other was seamless. Results from fixed-end burst tests at 170°C showed that the tube with the simulated weld had a burst strength of about 510 MPa and a hoop strain of about 1% at burst, with the rupture being confined to the weld. The seamless tube withstood a hoop stress greater than 570 MPa and a hoop strain greater than 2% without rupture. The tube did not burst, but failed at the weld between the tube and one flange in the fixed-end burst test fixture. These results confirm that the weld is the weakest part of the tube in biaxial stressing, and support the idea that the burst strength will be increased with a seamless tube.

3. Welds in Zr-2.5Nb

3.1 Delayed Hydride Cracking (DHC)

To prevent DHC in Zr-2.5Nb, one of the following risk factors must be absent [6,7]:

- hydrides; the hydrogen concentration must be less than the solubility limit, so that brittle hydrides do not form,
- tensile stress; the total stress and its amplification by flaws must be less than the critical value to fracture hydrides, and
- time; the duration of exposure to the first two risk factors must be minimised.

The critical stress and the susceptibility to DHC are characterised by K_{IH}, the threshold stress intensity factor. The microstructure of the material affects DHC properties, but K_{IH} appears to be dominated by crystallographic texture [8]. A common habit plane for hydride precipitates is close to the basal plane and this tends to be the cracking plane. Thus high tensile stresses parallel to basal plane normals should be avoided.

3.2 Experience with Welds

Experience with welded Zr-2.5Nb (ASTM Grades R60705 and R60901) has been mixed:

- The welds between the end caps and fuel sheathing in experimental fuel elements cracked in the heat-affected zone (HAZ) during storage at room temperature [9]. A heat-treatment of 530°C for 15 min and a modification to the design to reduce stress risers appeared to solve the problem.
- Similar cracking at room temperature was experienced in gas tungsten arc (GTA) welds in structures used in chemical processing [7]. In one example, the cracking was initiated by an oxygen-rich layer within five months of fabrication, while in

another, cracking was discovered about eighteen months after welding. Cracks followed the boundary between the HAZ and the fusion zone (FZ) of the weld.

- In 1986 the Tennessee Valley Authority installed two welded pressure vessels made from Zr-2.5Nb for the hydrolysis of wood fibers to produce ethanol. Both vessels were heated to 565±10°C for 1 h within 14 days after welding. The closure door on one vessel could not be heat treated, because of possible warpage. Consequently, the inside face was loosely clad with commercially pure zirconium (ASTM Grade R60702) and held in place with zirconium stud bolts that were sealed by welding. The units were batch operated at 215±10°C and 2.8 MPa for up to 20 h. After 40 cycles of operation and about 1.5 years after welding, the closure door began to leak. The stud bolt seal welds had cracked by DHC. The zirconium bolts were Zr-2.5Nb, rather than pure zirconium. Because the welds had not been stress relieved, they were subject to DHC. The bolts were replaced with pure zirconium and the vessel went back into service. All of the equipment has been in use for five years without further failure in any of the welds.

- A loop tube for WR-1, a research reactor at Whiteshell Laboratories, made from Zr-2.5Nb, contained five GTA welds. Within a few days of welding being completed, but over a month after the first weld was done, the tube was heat-treated at 400°C for 24 h, and within five months of welding the loop was operating at 230°C. Subsequent operation was at temperatures between 250°C and 300°C. The tube functioned without problems for the next eleven years, during which time the tube was at room temperature for 33 000 h. The welds received a low dose of neutrons - about 10^{23} n/m^2. No cracking was observed during post-irradiation examination of the welds.

- Electron-beam welding appears less harmful than GTA welding. Seven loop tubes for NRU, a research reactor at Chalk River Laboratories, contained 20 welds between Zr-2.5Nb and itself, Zircaloy-2 or Excel. These tubes were stored at room temperature for times up to 22 months before operating successfully at temperatures in the range 260°C to 300°C. Again, no cracking was detected during post-irradiation examination.

- A similar tube for an out-reactor loop contained two circumferential electron-beam welds, one of which cracked in the axial direction 16 months after welding. The weld was redone; the tube was operating at 250°C within two months of welding and performed without incident for eight months.

- The end caps of biaxial creep capsules were attached by electron beam welding, and then heat-treated at 400°C for 24 h within a few hours of welding [10]. Despite internal pressurization, none of the capsules has failed by DHC.

- None of the 50 000 electron beam welds between the diffusion joints and the main body of the pressure tube in RBMK reactors has suffered DHC after up to 16 years of reactor operation [11]. These welds were heat-treated at 580°C for 10 h within a few days of welding. To date, these welds have been irradiated to about 5×10^{22} n/m^2.

These examples illustrate the application of the risk factors. The failures occurred after extended periods at room temperature after welding. Hydrides are always present during storage at room temperature, because the solubility limit is less than 0.01 at% (1 ppm).

Reducing the hydrogen concentration below the solubility limit at room temperature is impractical, and thus this risk factor is always present. Once a component is operating at high temperatures this risk factor disappears, because the hydrogen is all in solution. For example, a component with an initial hydrogen concentration of 0.10 at% (10 ppm) will contain no hydrides at temperatures above 170°C. Also, the risk factor associated with stress will decline, because residual stresses will start to relax at elevated temperatures. Heat-treatment is effective in reducing residual stresses. No weld that was heated above 400°C soon after welding has failed. Thus an effective antidote to the stress risk factor is to stress relieve by heat-treatment before cracking can start.

3.3 Stress Relief

To estimate the time at temperature required to minimise cracking, we need to know:

- the maximum depth of surface flaw, a, that can be tolerated, which is estimated from [12]

$$a = C\left(\frac{K_{IH}}{\sigma}\right)^2 \qquad (4)$$

  where the shape factor C is about 0.4.

- the potential reduction in stress by stress relaxation.

As an illustration, we assume the as-welded residual tensile stress is the yield stress of Zr-2.5Nb annealed at 730°C for 1 h, and calculate the change in stress and critical flaw size from the unrelaxed stress ratio[1] and Equation (4), assuming that K_{IH} is 4.5 MPa$\sqrt{m}$. The results, summarised in Table II, show that a heat-treatment at a moderate temperature (400 to 450°C) can increase the critical flaw size by factors of three to ten, while an extra 50°C reduces the residual stress to 15% of its initial value and increases the critical flaw size by a factor of over forty. These results agree with experience. To confirm the analysis and understand why the cracks initiate in the HAZ, we have evaluated by neutron diffraction the texture and residual strains in welded Zr-2.5Nb plates.

3.4 Measurement of Texture and Residual Stress

Plates of Zr-2.5Nb, 6 mm thick, 190 mm wide and 300 mm long, were made by hot-rolling at 750°C followed by annealing at 730°C for 1 h. The plates were welded together in pairs perpendicular to the rolling direction using GTA welding. One set was left as-welded, while three others were heated to either 530, 590 or 650°C for 1 h.

3.4.1 Texture

To measure texture, specimens were cut from the fusion zone (FZ) and from the region of the HAZ with large prior-β grains, Figure 3. The specimens had dimensions of 30 mm parallel to

---

[1] Causey, A.R., Private communication, Atomic Energy of Canada Ltd., Chalk River Laboratories, 1993.

the long axis of the weld, 6 mm normal to the plate and 4 mm transverse to the weld. A third sample of base metal (BM) was obtained far from the weld.

The data are presented as pole figures in Figure 4. There are remarkable differences in the textures observed in the BM, HAZ and FZ, Figures 4 (a), (b) and (c), respectively. In the HAZ there is a pronounced maximum in the density of basal plane normals in the rolling direction. Hydride platelets will tend to precipitate on the normal-transverse plane, which accounts for the susceptibility of the HAZ to cracking parallel to the weld in the HAZ.

Heating for 1 h at 650°C effected a qualitative change in the texture of the FZ; it had no effect on the textures of the HAZ and BM. In Figure 4(c), eight markers (⊠) indicate the ideal positions of the {110} family of reflections in a cube texture. The cube texture is expected to develop during solidification from the melt into the high-temperature (bcc) phase of zirconium [14]. The [110] direction transforms into the [0002] direction on subsequent cooling into the low-temperature (hcp) phase [15]. In the as-welded FZ, all of the transformation variants are present, but in the FZ that was heat-treated at 650°C, the variants at the circumference of the pole figure (χ = 90°) have vanished, Figure 4(d). Unlike the heat-treatment at 650°C, those at the two lower temperatures had no effect on the weld textures.

Figures 4(e) to 4(g) present the $(10\bar{1}0)$ pole figures from the BM, HAZ and FZ of the as-welded plate, respectively. In the HAZ, wherever there is a high intensity in the (0002) pole figure (Figure 4(b)), there is a corresponding high intensity in the $(10\bar{1}0)$ pole figure (Figure 4(f)). Grain interaction stresses are expected in the HAZ [16].

3.4.2 Spatial Mapping of Texture Variations and Lattice Strains

Because of the variation in texture associated with the weld, no single diffraction peak could be chosen to determine the lattice strains over the area of interest. As the base metal has a strong transverse texture (Figure 4(a)) the strains in the rolling (RD), transverse (TD) and normal (ND) directions were calculated from the respective shifts in $(10\bar{1}0)$, (0002) and $(11\bar{2}0)$ peaks. In the HAZ and FZ, different diffraction peaks were required to obtain measurable signals. For the HAZ of the as-welded plate, the intensities of reflections from $(10\bar{1}0)$ and (0002) planes normal to the rolling direction are presented in Figure 5. The $(10\bar{1}0)$ intensity drops precipitously on entering the HAZ, which extends to a distance of about 13 mm from the centre of the weld. The $(10\bar{1}0)$ intensity is too low to determine a strain value for distances less than 12 mm from the centre of the weld. However, the intensity of the (0002) peak increases on entering the HAZ, and reaches a maximum at the fusion line. Thus rolling-direction strains within the HAZ could be determined from shifts in the (0002) diffraction peak. In the FZ, intensities of Bragg reflections exhibited an erratic dependence on position and the calculated strains displayed large fluctuations. Therefore, only the strains obtained in the base metal and HAZ are presented in this paper.

In Figure 6, the intensity of (0002) reflections is plotted against position. The intensities for the heat-treated plates have been normalized to coincide with the average of the intensities for the as-welded plate at 8, 10 and 12 mm from the weld centre. The normalized profiles are represented reasonably well by a single curve, and thus heat-treatment does not appear to influence the density of grains with (0002) normal to the rolling direction in the HAZ. The volume-averaged (0002) texture of the HAZ, Figure 4(b), revealed the undesirable tendency for basal plane normals to be oriented perpendicular to the weld direction; but now it can be concluded that this crystallite orientation is pronounced at the boundary between the HAZ and FZ, where the cracks develop in a weld.

Heat-treatment is very effective in relieving the macroscopic residual stresses. This is evident in Figure 7, where the TD, RD and ND strain components in the base metal are compared for the plates (a) as-welded and (b) heat-treated at 530°C for 1 h. In the as-welded plate, the dominant strain is parallel to the long dimension of the weld. The TD strain profile, which exhibits a high tensile value near the weld and an oscillation through a complementary compressive minimum about 30 mm from the weld centre, is expected to arise from the constrained shrinkage of the hot zones of the weld against the remainder of the base metal [17], and has been observed previously by neutron diffraction in a steel weld [18]. The ND and RD strains are approximately equal to each other and are mainly the Poisson's-ratio responses to the underlying TD stress field. After heat-treatment, the amplitude of the TD strain profile is reduced by about a factor of three, showing that the residual stress due to welding is relieved to a large extent.

Heat-treatment at 530°C did not reduce the component of strain in the RD in the HAZ, Figure 8. The pole figures of the HAZ show that in neighbouring grains [0002] and <10$\bar{1}$0> may be parallel, Figures 4(b) and 4(f). The coefficient of thermal expansion (CTE) along [0002] is about twice as great as that along <10$\bar{1}$0>. When the HAZ cools to room temperature, the difference in CTEs leaves [0002] in tension and <10$\bar{1}$0> in compression. The resulting stresses, called grain-interaction stresses, are not relaxed during heat treatment; they will remain at a level that depends on the relative volume fractions of the grains of each orientation. It follows that the component of strain in the rolling direction in the HAZ results from grain-interaction stresses.

3.5 Application

To achieve approval for the use of ASTM Grade R60705 (Zr-2.5Nb) in Section VIII of the American Society of Mechanical Engineers (ASME) Boiler and Pressure Vessel Code, a test program was initiated for the mitigation of DHC in welds. Four tests were conducted on samples cut from 9 mm thick plate of ASTM Grade R60705 annealed at 700°C for 1 h and filler welded into T-test plates. Two samples were heat treated at 566±10°C for one h at temperature 14 days after welding. The T-section samples, Figure 9, were subjected to static bending at room temperature in a three-point bend fixture. The outer fibre stress at the welds was estimated to be 80% of the yield strength of the plate material. The first sample to break was non-heat-treated and ruptured after 35 days, and the second non-heat-treated plate cracked after 14 months. The two heat-treated samples have not cracked in seven years of testing.

On the basis of the cracking experience, and the various analyses and experiments, the Boiler and Pressure Vessel Code of the ASME (Section VIII, Division I, Subsection C, UNF-56, (d), 1992, p. 183) now provides guidelines for time at temperature within a time after welding, as well as cooling rates to avoid large temperature gradients in thick-walled structures:

> "Within 14 days after welding, all products of zirconium Grade R60705 shall be heat-treated at 1000°F-1100°F (538°C-593°C) for a minimum of 1 h for thicknesses up to 1 in. (25.4 mm) plus 1/2 h for each additional inch of thickness. Above 800°F (427°C), cooling shall be done in a closed furnace or cooling chamber at a rate not greater than 500°F/h (260°C/h) divided by the maximum metal thickness of the shell or head plate in inches but in no case more than 500°F/h. From 800°F, the vessel may be cooled in still air."

For some applications this practice may be too restrictive. On a large vessel insufficient time may be available to meet the requirement of 14 days; a lower temperature of heat-treatment

may be more suitable to protect other metallurgical properties; or an electron beam weld may be less susceptible to DHC than a GTA weld. Future work will aim at reducing the conservatism built into the Code.

4. CONCLUSIONS

1. In the heat-affected zone of welds in zirconium alloy tubes or plates, the basal plane normals are rotated into the plane of the component and perpendicular to the direction of the weld.

2. For thin-walled Zircaloy-2 tubing containing an axial weld, the tube always fails in the weld when pressurised to failure in a fixed-end burst test. Reinforcing the weld by increasing its thickness by 25% moves the failure to the parent metal, improves the biaxial strength of the tube by 20 to 25%, and increases the total elongation by 200 to 450%.

3. In components made from Zr-2.5Nb, the texture in the heat-affected zone promotes DHC. Macro-residual tensile stresses can be relieved by heat-treatment (e.g., 530°C for 1 h), and therefore much reduce the probability of cracking. Large grain-interaction stresses remain as a result of mixed textures.

5. ACKNOWLEDGEMENTS

We would like to thank C.D. Cann, A.J. White, and R.M. Lesco for information on the performance of welds in tubes, and C.E. Ells for useful discussion. We would also like to thank K.V. Kidd, K. McCarthy, R.M. Condie and M. Cross for assistance with the experiments.

6. REFERENCES

[1] Ells, C.E., Coleman, C.E., and Chow, C.K., "Properties of a CANDU Calandria Tube," Canadian Metallurgical Quarterly, Vol. 24, 1985, pp. 215-223.

[2] Hill, R., "A Theory of the Yielding and Plastic Flow of Anisotropic Metals," Proceedings of the Royal Society, Vol. A 193, 1948, p. 281.

[3] Ells, C.E., Coleman, C.E., Hosbons, R.R., Ibrahim, E.F., and Doubt, G.L., "Prospects for Stronger Calandria Tubes," AECL-10339, Atomic Energy of Canada Ltd., Chalk River Laboratories, Chalk River, ON, 1990 December.

[4] Ernestus, A.W., U.S. Patent No. 3, 222,905, 14 Dec. 1965.

[5] Ernestus, A.W., U.S. Patent No. 3, 411,334, 19 Nov. 1968.

[6] Coleman, C.E., Cheadle, B.A., Ambler, J.F.R., Lichtenberger, P.C., and Eadie, R.L., "Minimising Hydride Cracking in Zirconium Alloys," Canadian Metallurgical Quarterly, Vol. 24, 1985, pp. 245-250.

[7] Cheadle, B.A., Coleman, C.E., and Ambler, J.F.R., "Prevention of Delayed Hydride Cracking in Zirconium Alloys," Zirconium in the Nuclear Industry: Seventh International Symposium, ASTM STP 939, R.B. Adamson and L.F.P. Van Swam, Eds., American Society for Testing and Materials, Philadelphia, 1987, pp. 224-240.

[8] Coleman, C.E., "Effect of Texture on Hydride Reorientation and Delayed Hydrogen Cracking in Cold-Worked Zr-2.5Nb," Zirconium in the Nuclear Industry: Fifth International Symposium, ASTM STP 754, D.G. Franklin, Ed., American Society for Testing and Materials, Philadelphia, 1982, pp. 393-411.

[9] Simpson, C.J. and Ells, C.E., "Delayed Hydrogen Embrittlement in Zr-2.5wt%Nb," Journal of Nuclear Materials, Vol. 52, 1974, pp. 289-295.

[10] Causey, A.R., Holt, R.A., Christodoulou, N.C., Elder, J.E., and Fleck, R.G., "On the Anisotropy of In-Reactor Creep of Zr-2.5Nb Tubes," This conference.

[11] Platonov, P.A., Ryazantseva, A.V., Frolov, I.A., Rodchenkov, B.S., Sinelnikov, L.P., and Eperin, A.P., "A Review of Investigations of RBMK Fuel: Control and Protection of Rod Channels for the 15 Years of Operation," This conference.

[12] Tiffany, C.F. and Masters, J.N., "Applied Fracture Mechanics," Fracture Toughness Testing and its Applications, ASTM STP 381, W.F. Brown, Jr., Ed., American Society for Testing and Materials, Philadelphia, 1965, pp. 249-277.

[13] Root, J.H. and Salinas-Rodriguez, A., "Neutron Diffraction Measurement of Texture Variations near a Weld in a Zr-2.5Nb Plate," Textures and Microstructures, Vol.14-18, 1991, pp. 989-994.

[14] Davies, G.J. and Garland, J.G., "Solidification Structures and Properties of Fusion Welds," International Metallurgical Reviews, Vol. 20, 1975, p. 83.

[15] Burgers, W.G., "On the Process of Transition of the Cubic-body-centered Modification into the Hexagonal-close-packed Modification of Zirconium," Physica, Vol. 1, 1934, pp 561-586.

[16] MacEwen, S.R., Tome, C., and Faber, J., "Residual Stresses in Annealed Zircaloy," Acta Metallurgica, Vol. 37, 1989, p. 979.

[17] Wohlfahrt, H., "Residual Stresses due to Welding: their Origin, Calculation, and Evaluation," Residual Stresses, E. Macherauch and V. Hauk, Eds., Informationsgesellschaft Verlag, Oberursel, 1986, pp. 81-112.

[18] Root, J.H., Holden, T.M., Schroeder, J., Hubbard, C.R., Spooner, S., Dodson, T.A., and David, S.A., "Residual Stresses in a Multipass Ferritic Weldment," Materials Science and Technology, in press.

TABLE I

DEVELOPMENT OF BIAXIAL STRENGTH IN ZIRCALOY-2 CALANDRIA TUBES: MEAN VALUE (RANGE)

Material	UTS, MPa			R	P	Burst Strength, MPa			
	Transverse		Longi-tudinal			As-received	Predicted From		Weld Reinforcement: Break in Parent Metal
	Parent Metal	Weld	Parent metal				Equation 1	Equation 2	
Sample 1: Basal planes 40° from radial direction, oxygen concentration 0.74 at% (1300 ppm)	320	350	350	2.5 (2-3)	4.4 (3.5-5.3)	535 (510-560)	577 (545-610)	493 (461-525)	675 (640-710)
Sample 2: Basal planes in radial direction, oxygen concentration 0.69 at% (1200 ppm)	305	360	320	5 (4-6)	5.5 (4.4-6.6)	550 (520-580)	595 (550-640)	560 (520-600)	665 (630-700)

TABLE II

STRESS RELAXATION AND CRITICAL FLAW SIZE FOR CRACKING[a]

Temperature, °C	Time, h	Unrelaxed Stress Ratio	Stress, MPa	Critical Flaw Size, mm
...	...	1.0	380	0.06
400	6.0	0.55	209	0.19
450	3.0	0.3	114	0.62
500	1.0	0.15	57	2.49
550	0.5	0.10	38	5.6

[a] Zr-2.5Nb annealed at 730°C for 1 h. At room temperature, the yield stress is 380 MPa.

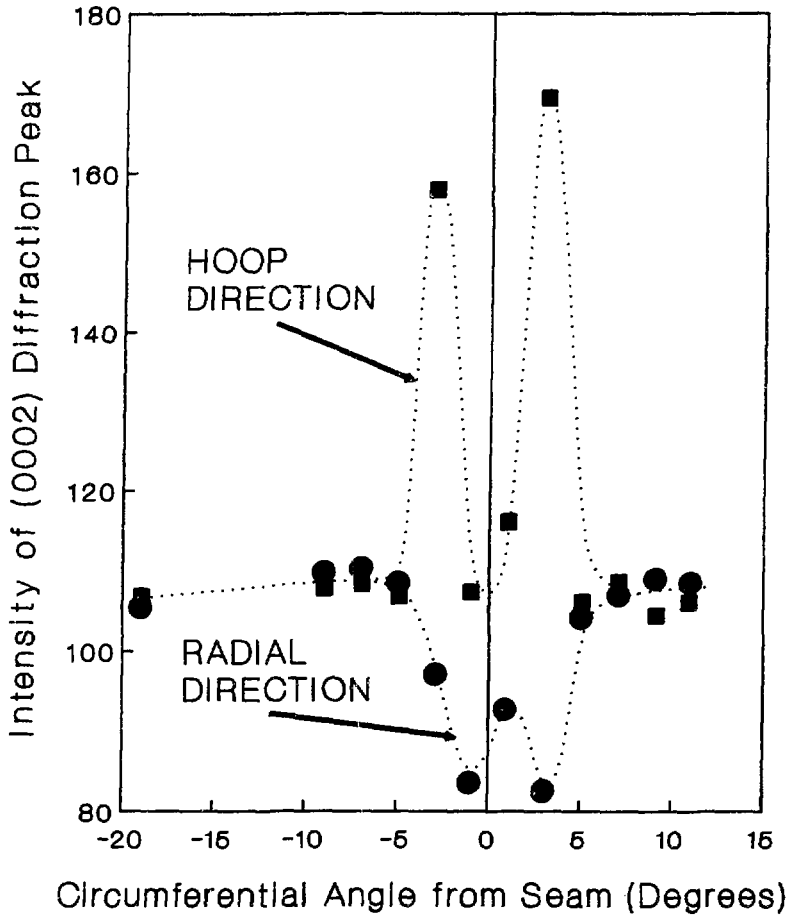

Figure 1: Variation in the density of (0002) poles in the radial and transverse directions near the seam weld in a Zircaloy-2 calandria tube.

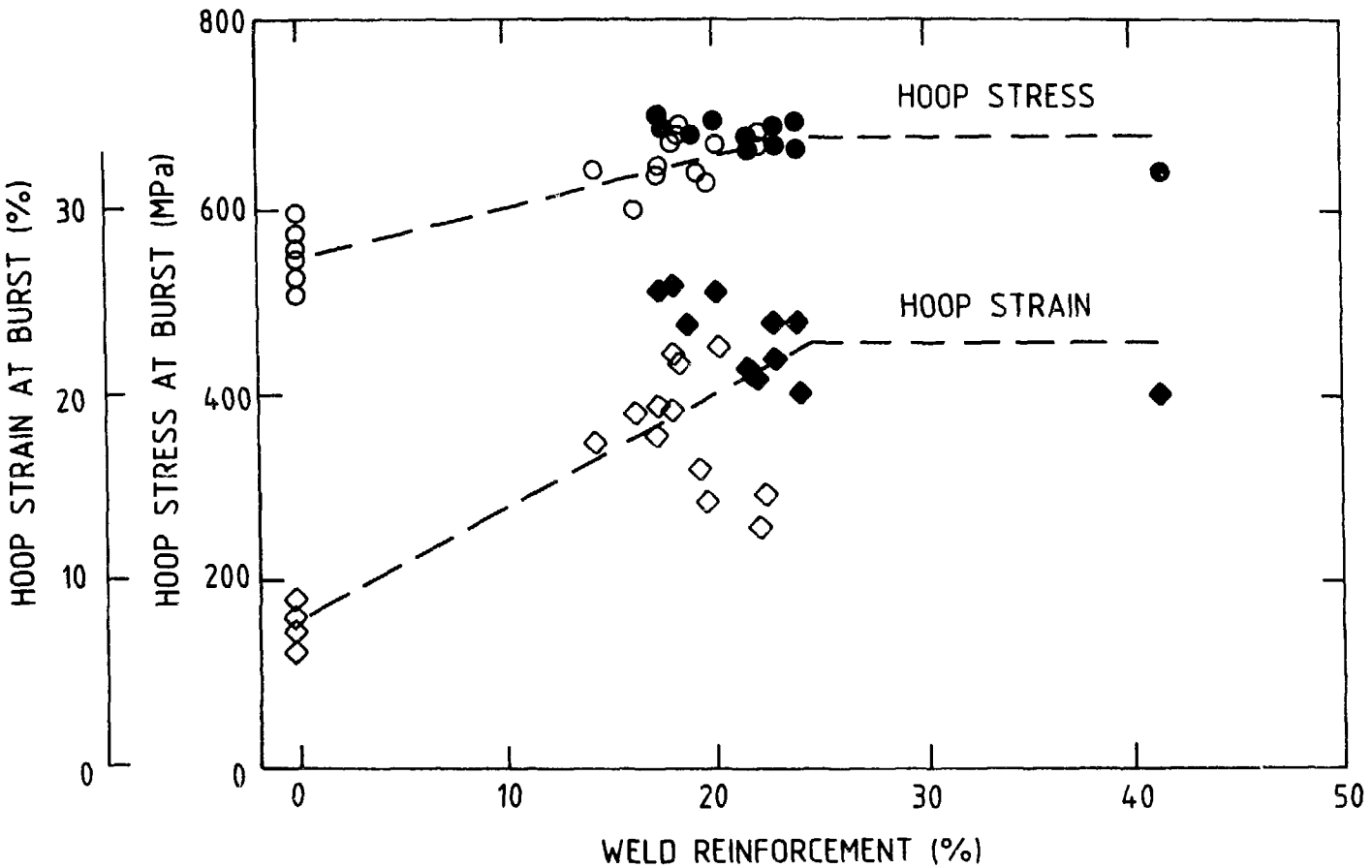

Figure 2: Dependence of hoop stress and strain at burst on the thickness of the seam weld in Zircaloy-2 calandria tubes. Filled symbols indicate rupture in the parent material.

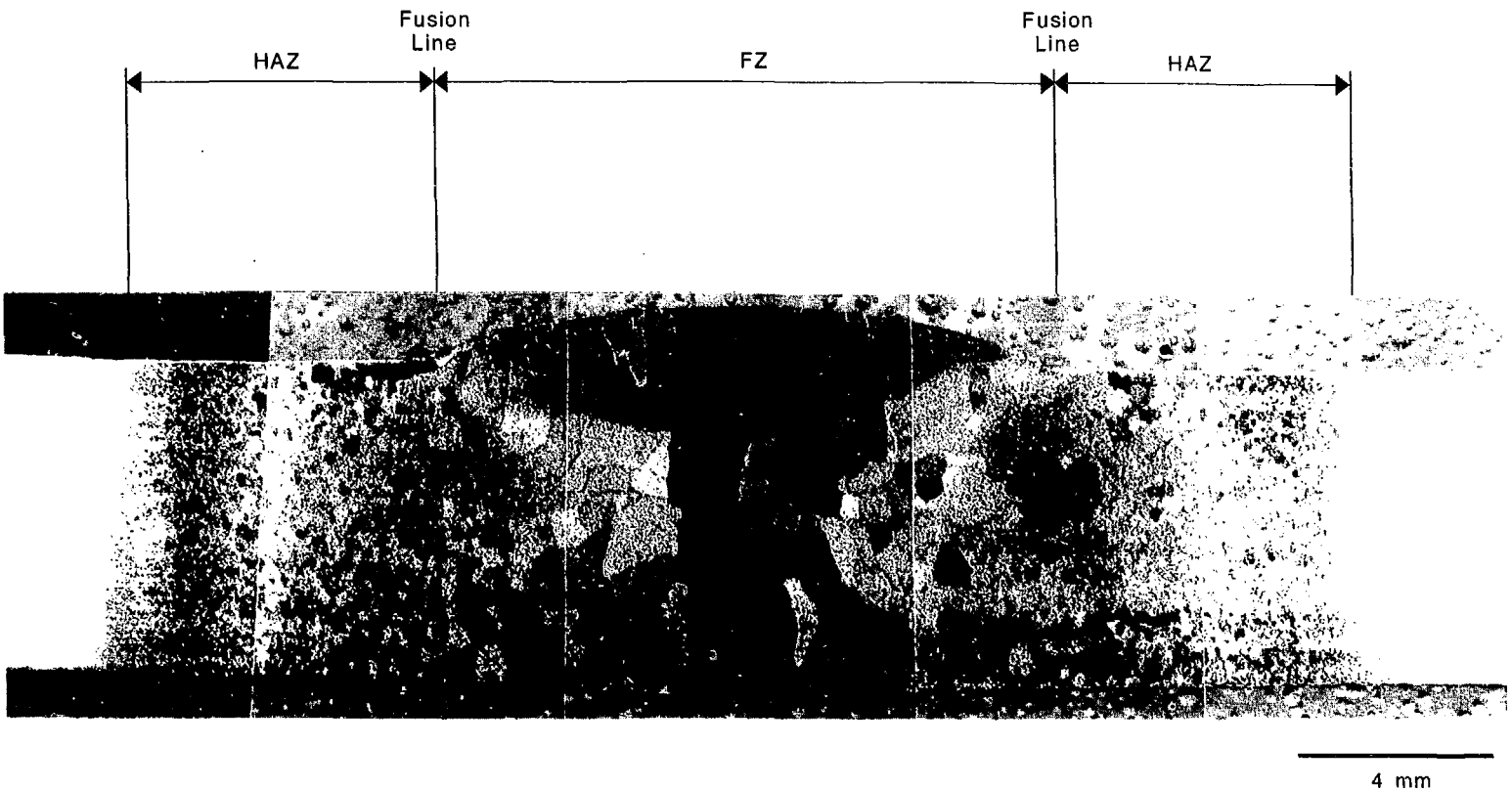

Figure 3: Macrostructure of a GTA weld between Zr-2.5 Nb plates.

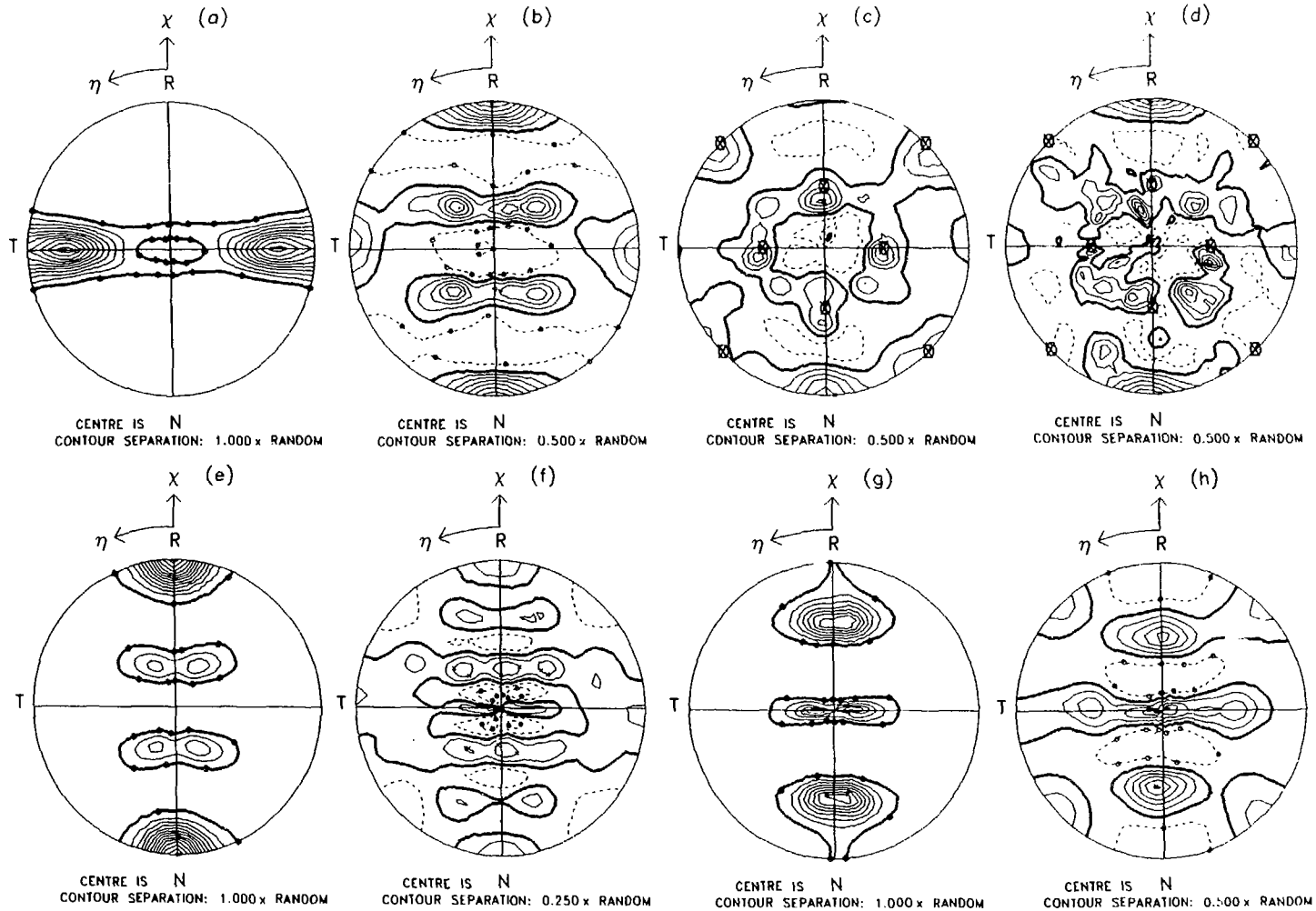

Figure 4: Pole figures of GTA welds between Zr-2.5Nb plates: (0002)--as-welded: (a) base-metal [13], (b) heat-affected zone [13], and (c) fusion zone [13]; welded and 650°C for 1 h: (d) fusion zone. ($10\bar{1}0$)--as-welded: (e) base-metal, (f) heat-affected zone, (g) fusion zone; welded and 650°C for 1 h: (f) fusion zone.

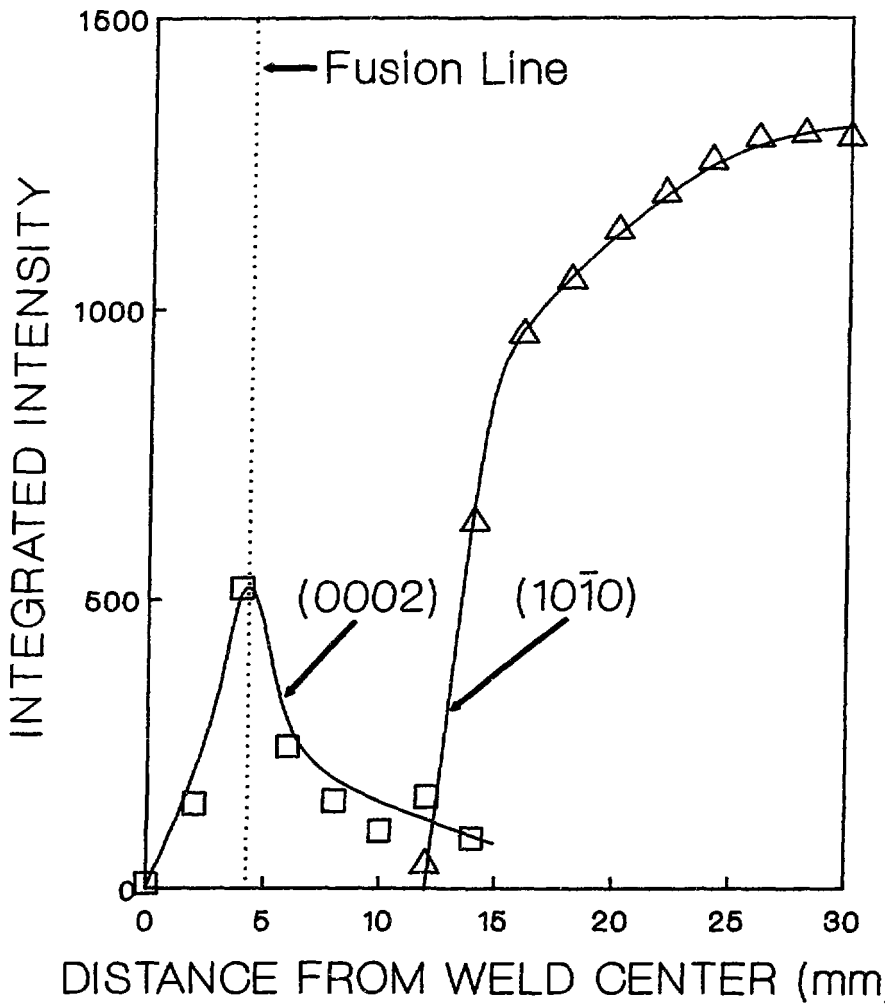

Figure 5: Variation in the densities of (0002) and (10$\bar{1}$0) poles with distance from the centre line of a GTA weld between Zr-2.5Nb plates.

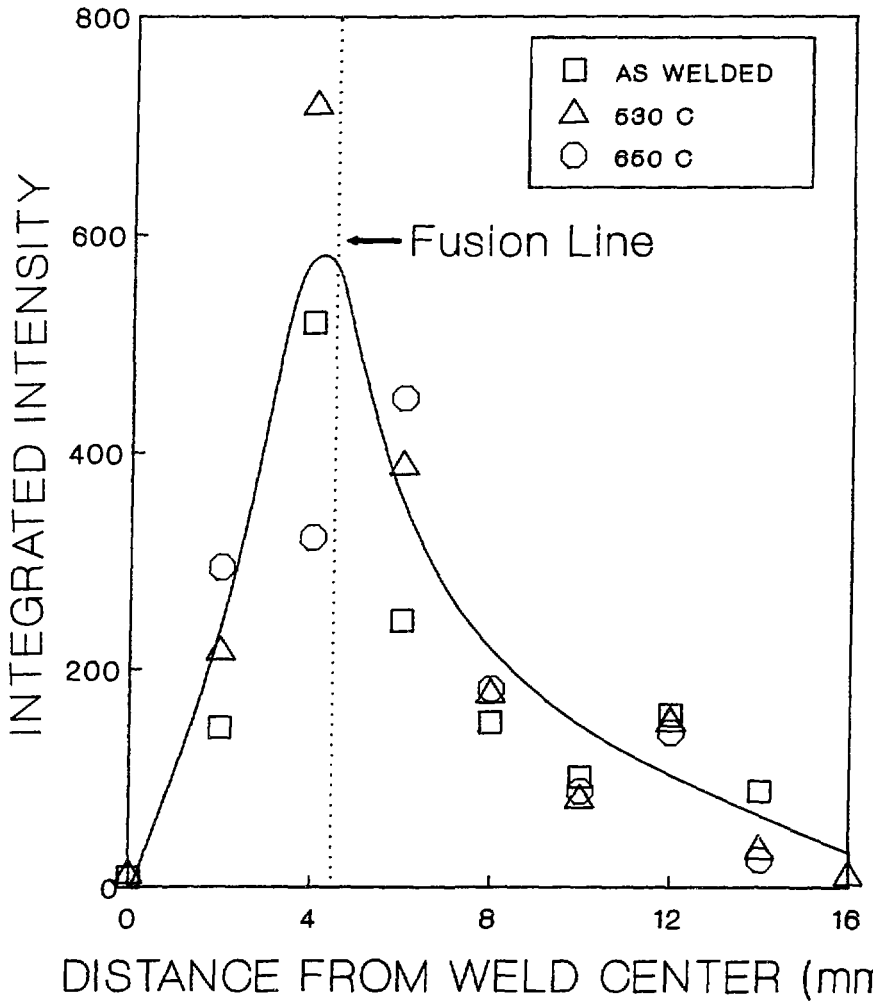

Figure 6: Variation in the density of (0002) poles with distance from the centre line of GTA welds between Zr-2.5Nb plates, before and after heat-treatment at 590 and 650°C.

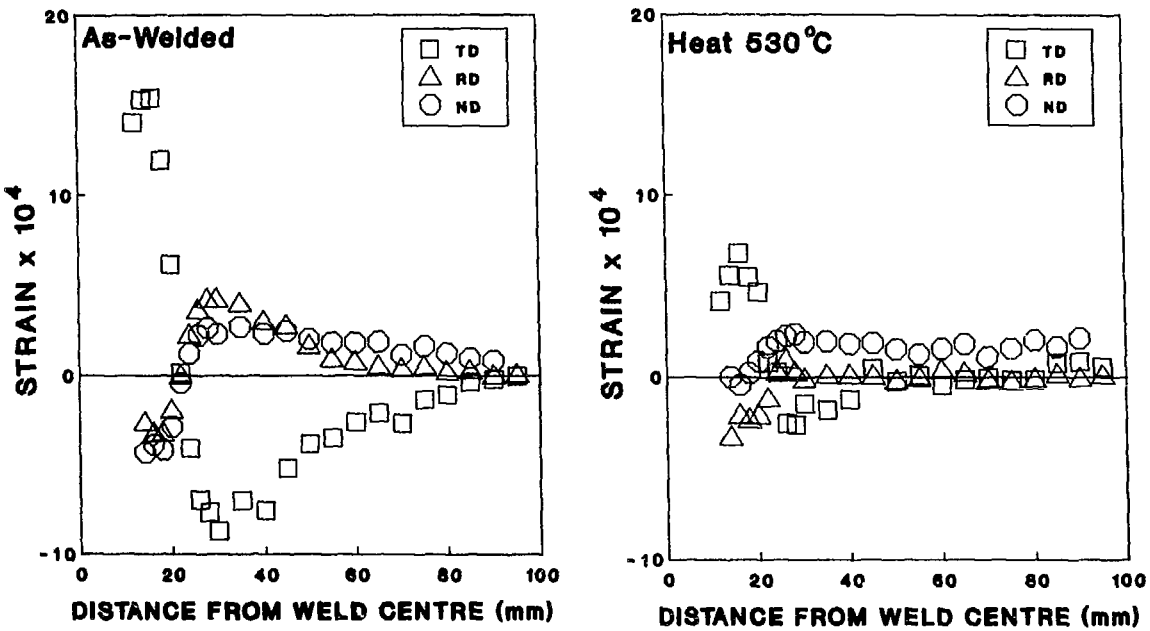

Figure 7: Distribution of residual strains in the transverse, rolling and normal directions in GTA welds between Zr-2.5Nb plates: (a) as-welded and (b) after heat-treatment of 530°C for 1 h.

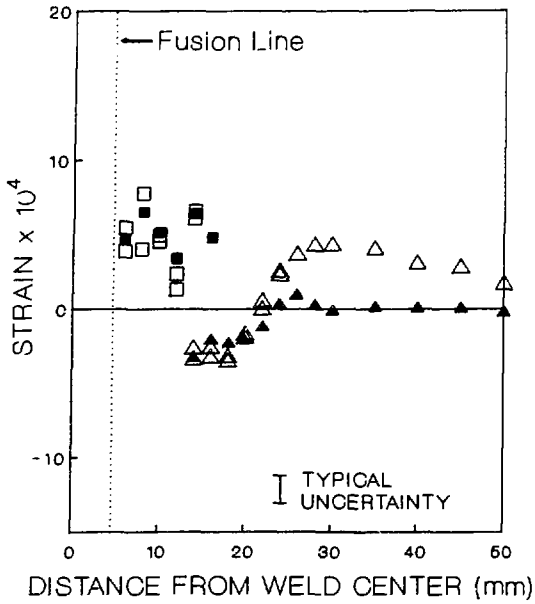

Figure 8: Distribution of residual strains in the rolling direction associated with GTA welds between Zr-2.5Nb plates: (0002)--□ as-welded and ■ heat treated for 1 h at 530°C; (10$\bar{1}$0)--△ as-welded and ▲ heat-treated for 1 h at 530°C.

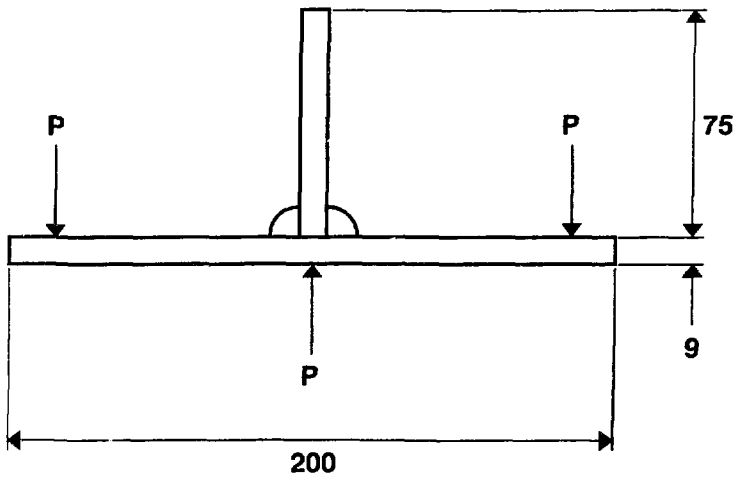

Figure 9: Welded T-sections used to test efficacy of heat-treatment to prevent DHC in Zr-2.5Nb. Dimensions are in mm.

APPENDIX A

Calandria Tube Fixed-End Burst Test

Fixed-end burst tests are conducted at 170°C to simulate reactor conditions in the event of pressure tube rupture. In Figure A.1, a burst test assembly is shown with both ends of the tube secured with a tie bar to restrict axial movement, usually contraction, of the internally pressurised tube. End-caps are welded to the tube to seal the ends, and clamps prevent the welded ends from breaking when the tube bulges. To measure axial and hoop strains, foil strain gauges are bonded to the tube at mid-length. Temperature is measured with type-K thermocouples attached to the tube. Burst tests were done in a steel bell jar. The sample is placed vertically inside the bell jar, heated to 170°C, and rapidly pressurized to failure. The pressure and circumference of the tube is measured at burst. Burst stress σ_H is given by:

$$\sigma_H = \frac{PD}{2t} \qquad \text{(A.1)}$$

where P is the maximum pressure in MPa, and D and t are, respectively, the instantaneous inside diameter and initial wall thickness of the tube in mm. The maximum hoop strain e_H in % at burst is written as:

$$e_H = \frac{c_f - c_i}{c_i} \times 100 \qquad \text{(A.2)}$$

where c_i and c_f are the initial and final circumferences of the tube.

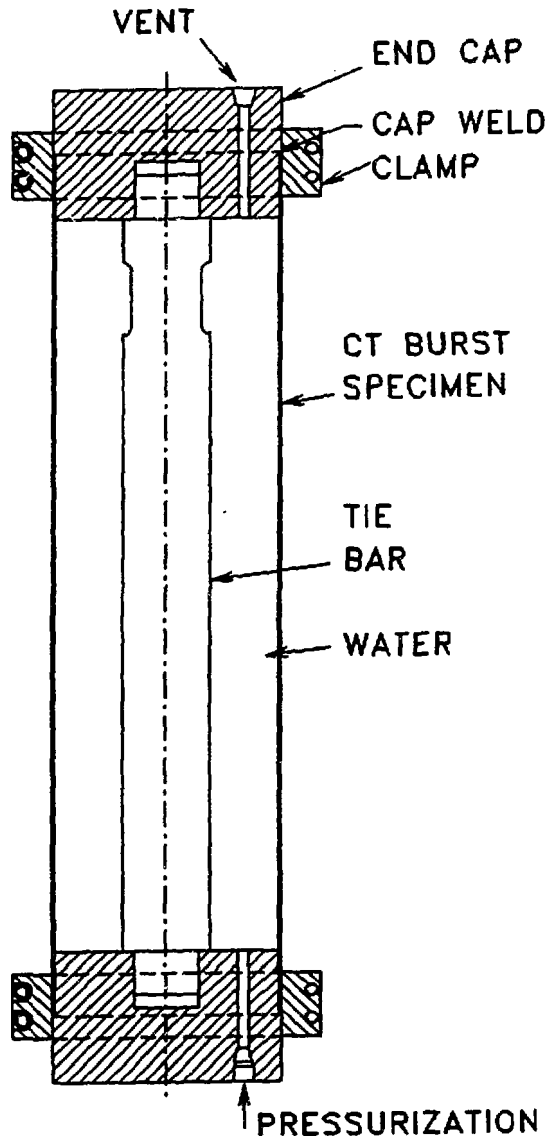

Figure A.1: Schematic diagram of fixed-end burst test apparatus.

APPENDIX B

Neutron Diffraction as a Probe of Texture and Strain Distributions in Zirconium-Alloy Welds

Neutrons penetrate easily through zirconium. A neutron beam is attenuated by 30% on traversing a thickness of 12 mm. Therefore, neutron diffraction can be used for non-destructive examination of engineering components. Two techniques are presented in this paper.

The first technique is the quantitative analysis of the crystallographic texture. To characterize the texture of a rolled plate, a specimen is made with one axis parallel to the normal direction. The angle χ is measured from the normal direction (N), while the angle η is measured counterclockwise from the rolling direction (R). A Eulerian cradle tilts the specimen through 90° in χ and rotates the specimen about its axis by 360° in η. For each direction in the specimen, (χ,η), measurements are made of the intensities of at least five neutron diffraction peaks, $(10\bar{1}0)$, (0002), $(10\bar{1}1)$, $(10\bar{1}2)$ and $(11\bar{2}0)$. The intensity is proportional to the volume fraction of crystallites with plane normals parallel to the direction (χ,η). The intensity variation of a particular diffraction peak is plotted on a stereogram. Contour lines connect points of equal intensity. Dashed lines indicate intensities less than those of a random distribution of crystallite orientations; continuous lines indicate intensities greater than those of a random distribution. A thick line indicates the intensity that would be observed if there were a completely random distribution of crystallite orientations in the material. The contour interval is quoted in multiples of the intensity of a random distribution. Because neutrons penetrate easily through the material, complete pole figures can be obtained with a single setting of a specimen on the Eulerian cradle. In all orientations, the full volume of the specimen is sampled by the neutron beam. Since neutrons probe the full volume of the specimen, many more grains are sampled than would occur in X-ray diffraction, which probes only a thin surface layer.

The second technique is the spatial mapping of texture and lattice strain. Both the incident and diffracted neutron beams can be shaped by rectangular slits in neutron-absorbing cadmium masks. The intersection of the incident and diffracted beams defines the sampling volume, typically of the order of $2 \times 2 \times 2$ mm^3, which can be set at various locations within a welded zirconium-alloy plate. The plate is moved by computer-controlled XYZ translators. At each location, a diffraction peak is measured. The raw data, neutron counts versus scattering angle, 2θ, are fitted with a model function, a Gaussian on a linear background, to obtain accurate measures of the integrated peak intensity and the mean value of 2θ. The peak intensity varies with location in a welded plate because the texture is strongly affected by the thermal history of each weld zone. The mean value of 2θ also varies with location, because welding produces a residual stress field that creates strains in the crystal lattices of the grains. By comparing the value of 2θ obtained at a particular location within the weld with the value $2\theta_o$ obtained from a specimen that is stress-free, the lattice strain ε can be deduced from the relation:

$$\epsilon = \frac{\sin\theta_o}{\sin\theta} - 1 \qquad \text{(B.1)}$$

Outside the FZ, the principal axes of the residual stress field are expected to be the symmetry directions of the rolled plate, the rolling (RD), transverse (TD) and normal (ND) directions. To determine the corresponding components of strain, these directions must each be placed

parallel to the bisector, as illustrated in Figure B.1. Because neutrons easily penetrate through zirconium alloys, direct measurements of lattice strain can be made without destroying the weld.

The wavelength of the neutron beam was 0.19005 nm, calibrated against a silicon powder specimen obtained from the National Institute of Standards and Technology. Strains were calculated from scattering angles at locations within the weld and those obtained from a reference specimen, a small rectangular coupon cut from a corner of the plate heat-treated at 650°C for 1 h.

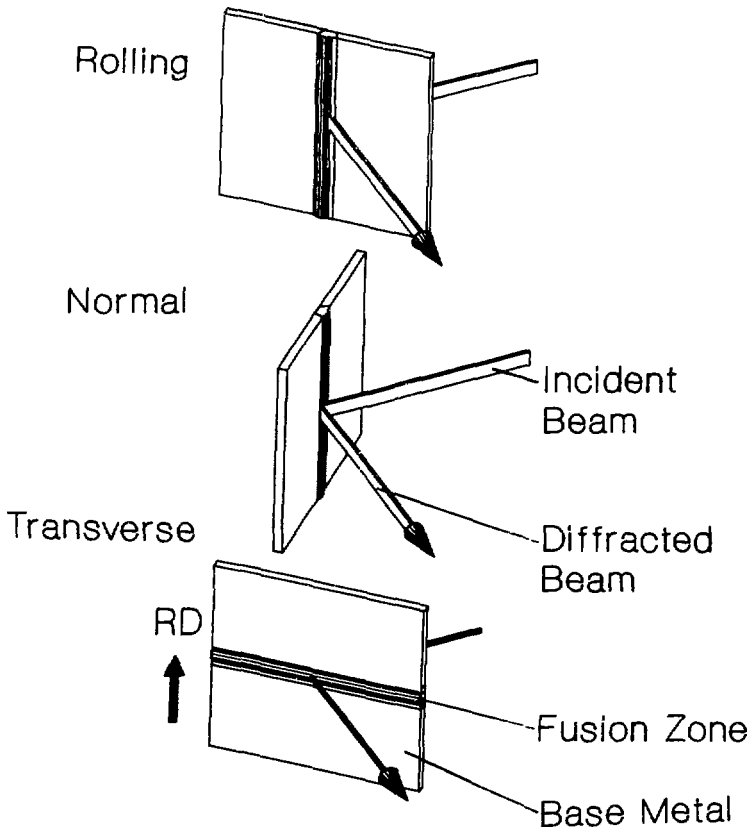

Figure B.1: Orientation of welded plate for the measurement of strain in the rolling, normal and transverse directions.

Cat. No. CC2-10950E
ISBN 0-660-15372-6
ISSN 0067-0367

To identify individual documents in the series we have assigned an AECL- number to each.

Please refer to the AECL- number when requesting additional copies of this document

from

Scientific Document Distribution Office
Atomic Energy of Canada Limited
Chalk River, Ontario, Canada
K0J 1J0

Price: A

No. au cat. CC2-10950E
ISBN 0-660-15372-6
ISSN 0067-0367

Pour identifier les rapports individuels faisant partie de cette série nous avons assigné un numéro AECL- à chacun.

Veuillez faire mention du numéro AECL- si vous demandez d'autres exemplaires de ce rapport

au

Service de Distribution des Documents Officiels
Énergie atomique du Canada limitée
Chalk River, Ontario, Canada
K0J 1J0

Prix: A

© ATOMIC ENERGY OF CANADA LIMITED, 1993

2546-93